第 5 卷　第 4 期　　航空动力学报　　Vol. 5　No. 4
1990 年　10 月　　Journal of Aerospace Power　　Oct.　1990

循环加载下的热弹塑蠕变有限元分析

西安交通大学　　穆霞英　胡志强

【摘要】　本文考虑在循环加载条件下，采用混合强化模型，导出相应的热弹塑性蠕变增量本构方程及有限元格式。研制出平面应力程序，用牛顿迭代法求弹塑性权，并提出精度高的屈服吸面校正方法，程序经考核，可供工程设计使用。

一、前　言

金属结构在高温环境下往往承受反复加载，于是材料表现出不同程度的鲍氏效应。考虑到材质变化与鲍氏效应，我们曾对变温变载下的混合强化模型提出探讨[1]。本研究顾及蠕变疲劳交互作用的寿命预测，需要对模拟试验件（平面应力问题）进行循环应力应变分析。为此，采用文献[1]的强化模型，推导相关联的热弹塑性蠕变增量本构方程及有限元计算公式，研制了循环加载下的平面应力程序，混合强化模型的热弹塑性蠕变分析程序，简称 MTEPCA。

程序结构按加载→蠕变→卸载（含反向加载）→蠕变→再加载，重复以上循环。程序采用子步增量法求应力，牛顿迭代法求弹塑性权系数以及精度较高的屈服面校正方法。对于弹塑性平面应力问题，$\Delta\alpha$ 及 $\Delta\epsilon$ 不为零的问题，进行了有效的处理。

二、混合强化模型

Hodge 提出的室温下的混合强化模型基本思想是由等向强化与随动强化两种模型的组合。文献[1]将这种思想推广到变温过程，并考虑到材质变化的影响。变温条件下塑性流动过程，混合强化模型有移动且伴随着均匀扩大（或缩小）。这可看作按运动强化模型作部分移动及按等向强化模型作部分均匀扩大（或缩小）。以 Von-Mises 型材料为例，其强化条件一般形式为：$f(\sigma_{ij}-\alpha_{ij})=\bar{H}^2(\bar{\epsilon}_p, M, T)$。其中，$\bar{H}$ 是瞬时屈服应力，它度量应力空间混合强化屈服面半径。σ_{ij}、α_{ij}、$\bar{\epsilon}_p$，及 T 各表示应力张量、屈服面中心的移动向量、等效塑性应变及温度。现在的问题是如何确定 $\bar{H}$？若以线性硬化材料为例，画出单向应力应变回线如图 1 所示。图中 I、II、III 表示随动强化、等向强化和混合强化模型所对应的回线，则存在图示关系：

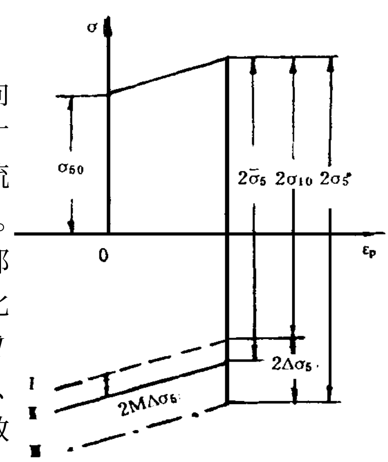

图 1　$\bar{H}$ 的确定

$$\bar{H}(\bar{\epsilon}_p, M, T)=\sigma_{so}+M\Delta\sigma_s=\sigma_{so}(1-M)+MH(\bar{\epsilon}_p, T)$$

式中，$\sigma_{so}=\sigma_{so}(T)$，表示当前温度的初始屈服应力，$H$ 表示等向强化模型的瞬时屈服强度。

本文于 1990 年 4 月收到。

这里 M 定义为强化参数，在变温条件下 $M = M(T)$，其变化范围 $0 \le M \le 1$。当 $M = 0$ 则 $\bar{H} = \sigma_{so}$ 为随动强化模型Ⅰ；当 $M = 1$ 时，$\bar{H} = H$，表示等强化模型Ⅱ。

在运算前 M 为已知，可以根据不同温度下材料的多级疲劳试验作到稳定循环，得到图 1 所示回线，即 $M = (\bar{H} - \sigma_{so})/(H - \sigma_{so})$ 确定 M 并建立函数关系 $M(T)$。

三、增量本构关系及有限元计算公式

本构模型采用文献 [2] 所述，总应变增量为

$$d\epsilon_{ij} = d\epsilon_{ij}^{e} + d\epsilon_{ij}^{p} + d\epsilon_{ij}^{c} + d\epsilon_{ij}^{T} \tag{1}$$

式中各分量具有上标 e、p、c、T 者各表示弹性、塑性、蠕变、热应变的增量。

加载面具体表达式采用　$f(\sigma_{ij} - \alpha_{ij}) = (1/2)s_{ij}s_{ij} - (1/3)\bar{H}^2 = 0$　(2)

$$s_{ij} = \sigma_{ij} - \alpha_{ij} - (1/3)\delta(\sigma_{kk} - \alpha_{kk})$$

塑性流动按正交性法则　$d\epsilon_{ij}^{p} = (\partial f/\partial \sigma_{ij})d\lambda$　(3)

按照混合强化模型思想，塑性应变增量 $d\epsilon_{ij}^{p}$ 由两部分组成，即

$$d\epsilon_{ij}^{p} = d\epsilon_{ij}^{p(i)} + d\epsilon_{ij}^{p(k)} \tag{4}$$

式中 $d\epsilon_{ij}^{p(i)}$、$d\epsilon_{ij}^{p(k)}$ 分别描述加载面按等向强化及随动强化模型相关的塑性变形部分。

而　$d\epsilon_{ij}^{p(i)} = M d\epsilon_{ij}^{p}$，　$d\epsilon_{ij}^{p(k)} = (1 - M)d\epsilon_{ij}^{p}$　(5)

若随动强化按 Prager 假设

$$d\alpha_{ij} = c d\epsilon_{ij}^{p(k)} = 2[(\partial H/\partial \bar{\epsilon}_p) + (\partial H/\partial T)(dT/d\bar{\epsilon}_p)](1 - M)d\epsilon_{ij}^{p}/3 \tag{6}$$

其中 c 由单向拉伸曲线 $\sigma = H(\bar{\epsilon}_p, T)$ 确定。考虑到 $d\epsilon_{ij}^{c}$、$d\epsilon_{ij}^{T}$ 等应变增量可推得增量本构方程。

$$d\sigma_{ij} = (D_{ijkl} - D_{ijkl}^{p})(d\epsilon_{kl} - d\epsilon_{kl}^{o}) + d\sigma_{ij}^{o} \tag{7}$$

仅当 $L = (\partial f/\partial \sigma_{ij})d\sigma_{ij} + (\partial f/\partial T)dT > 0$ 时发生塑性流动。

塑性区的本构方程 (7) 可写成有限元格式，考虑到过渡区，一般形式为:

$$\Delta\{\sigma\} = (1 - r)[\bar{D}]_{ep}(\Delta\{\epsilon\} - \Delta\{\epsilon\}^{o}) + \Delta\{\sigma\}^{o}] + r\Delta\{\sigma\}^{e} \tag{8}$$

而　$[\bar{D}]_{ep} = [D] - (1 - r)[\bar{D}]_{p}$　(9)

这里，$\Delta\{\sigma\}^{e}$、$[\bar{D}_{ep}]$、r 各表示相应于 $(\Delta\{\epsilon\} - \Delta\{\epsilon\}^{o})$ 的弹性应力增量、加权弹塑性矩阵及弹塑性权系数 $(0 \le r \le 1)$。当 $r = 1$ 单元为弹性区，$r = 0$ 为塑性区，$(0 < r < 1)$ 为过渡区。

在平面应力状态下可推得有限元具体算式

$$[\bar{D}]_{p} = \frac{E}{(1 - \mu^2)g}\begin{bmatrix} (S_x + \mu S_y)^2 & (S_y + \mu s_y)(S_y + \mu S_x) & (1 - \mu)(S_x + \mu S_y)s_{xy} \\ (S_y + \mu s_y)(S_y + \mu S_x) & (S_y + \mu S_x)^2 & (1 - \mu)(S_y + \mu S_x)S_{xy} \\ (1 - \mu)(S_x + \mu S_y)s_{xy} & (1 - \mu)(S_y + \mu S_x)S_{xy} & (1 - \mu)^2 s_{xy}^2 \end{bmatrix} \tag{10}$$

$$g = [S_x^2 + S_y^2 + 2(1 - \mu)S_{xy}^2 + 2\mu S_x S_y] + [(4H'/3)(1 - M)(S_x^2 + S_y^2 + S_x S_y + S_{xy}^2)$$
$$+ (4/3\sqrt{3})\bar{H}(\partial \bar{H}/\partial \bar{\epsilon}_p)(S_x^2 + S_y^2 + S_x S_y + S_{xy}^2)^{1/2}](1 - \mu^2)/E \tag{11}$$

$$\Delta\{\sigma\}^{o} = (1/g)[(2\bar{H}/3)(\partial \bar{H}/\partial T)dT + (1 - M)(2/\sqrt{3})(S_x^2 + S_y^2 + S_x S_Y + S_{xy}^2)^{1/2}$$
$$\cdot(\partial H/\partial T)dT]\{S_x + \mu S_y, \mu S_x + S_y, (1 - \mu)S_{xy}\}^{T} \tag{12}$$

$$\Delta\{\tilde{\epsilon}\} = \begin{Bmatrix} \alpha - (1/E^2)(dE/dT)\sigma_x + [(\mu/E^2)(dE/dT) - (1/E)(d\mu/dT)]\sigma_y \\ \alpha + [(\mu/E^2)(dE/dT) - (1/E)(d\mu/dT)]\sigma_x(1/E^2)(dE/dT)\sigma_y \\ \{-[(1 + \mu)/E^2](dE/dT) + (1/E)(d\mu/dT)\}2\tau_{xy} \end{Bmatrix} \tag{13}$$

$$\Delta\{\tilde{\epsilon}\}^o = \Delta\{\tilde{\epsilon}\} + \Delta\{\epsilon\}^c \tag{14}$$

在塑性区除了满足本构方程 (8)，还要满足平衡关系

$$[K]_{ep}\Delta\{\delta\} = \Delta\{p\} + \Delta R\{\Delta\{\epsilon\}^o\} + \Delta R\{\Delta\{\sigma\}^o\}\quad,\quad [K]_{ep} = \int [B]^T[D]_{ep}[B]dv \tag{15}$$

$$\Delta\{R(\Delta\{\epsilon\}^o)\} = \int [B]^T[D]_{ep}\Delta\{\epsilon\}^o dv\quad,\quad \Delta\{R(\Delta\{\sigma\}^o)\} = \int [B]^T\Delta\{\sigma\}^o dv \tag{16}$$

四、计算方法的新改进

1. 弹塑性权系数计算 过渡区权系数 r 的算法，一般以前一增量步的 r 值计算本步，但增量要求很小。这里改进为采用本步内牛顿迭代法，精度高、工作量小。其基本思想方法是，设在增量步的初与末，应力点 A 及 B 处于弹性状态与塑性状态，则必存在不等式 $f(\{\sigma\}_A) = f_A < 0, f(\{\sigma\}_A + \Delta\{\sigma\}^e) = f_B > 0$。设其间 c 点刚好进入屈服，则

$$f(\{\sigma\}_c) = f(\{\sigma\}_A) + r\Delta\{\sigma\}^e = f_c = 0 \tag{17}$$

若利用 f_A，f_B 值进行线性插值可得到 r_1，但不一定满足 (17) 式，需再对 r_1 作进一步修正即

$$f(\{\sigma\}_A + (r_1 + \Delta r_1)\Delta\{\sigma\}^e) = 0 \tag{18}$$

用泰勒级数展开只保留一次项，得

$$\Delta r_1 = -f_c/[\{\partial f/\partial\{\sigma\}\}^T\Delta\{\sigma\}^e] \tag{19}$$

于是可得精确求解弹塑性权系数 r 的迭代公式:

$$f_i = f(\{\sigma\}_A + r_i\Delta\{\sigma\}^e)\quad,\quad r_{i+1} = r_i - f_i/[\{\partial f/\partial\{\sigma\}\}^T\Delta\{\sigma\}^e] \tag{20}$$

这里以 $r_1 = -f_A/(f_B - f_A)$ 为初值进行迭代，直到所需精度为止。

2. 子步内屈服面校正 为减少本构方程因线性化处理引起的误差，在计算 $\Delta\{\sigma\}$ 时采用子步增量法。按此法计算往往在增量步末，现时应力不一定满足硬化规律。需要进行屈服面校正，修正应力使应力点落在屈服面上。但现有方法往往因为应力的修正，又引起流动法则的不满足。为此本文设想在增量步内应变增量保持不变，对应力、屈服面半径同时进行修正，使每一子步末，流动法则、硬化条件同时得到满足的方法来修正应力。假设子增量步内应变增量

的值不变，即

$$\delta\{\epsilon\} = \delta\{\epsilon\}^e + \delta\{\epsilon\}^p = 0 \tag{21}$$

每一子步末，若应力点 B 不满足硬化条件，即 $f_B = F(\{\sigma\} + \Delta\{\sigma\}^i - \{\alpha\} - \Delta\{\alpha\}^i) - (1/3)\bar{H}_i^2 \neq 0$，式中上标 i 表示第 i 个子步。对 f_B 作用微增量 $\delta\{\sigma\}$，$\delta\{\alpha\}$，$\delta\bar{H}$，让 $f = 0$，即

$$f_c = F(\{\sigma\} + \Delta\{\sigma\}^i + \delta\{\sigma\} - \{\alpha\} - \Delta\{\alpha\}^i) - \delta\{\alpha\}(1/3) - (\bar{H}_i + \delta\bar{H})^2 = 0$$

展开上式取一次项，以 (3)、(6) 及 (21) 式代入，可得

$$d\lambda = f_B/[\{\partial f/\partial\sigma\}^T[D]\{\partial f/\partial\sigma\} + (2/3)(1-M)(\partial H/\partial\bar{\epsilon}_p)\{\partial f/\partial\sigma\}^T\{\partial f/\partial\sigma\} + (2/3)\bar{H}_i(\partial\bar{H}/\partial\bar{\epsilon}_p)((2/3)\{\partial f/\partial\sigma\})^T\{\partial f/\partial\sigma\})^{1/2}] \tag{22}$$

在计算中考虑到增量步内材质变化是固定的，进行屈服面校正时 $dT = 0$，应力修正时屈服面半径的变化仅由塑性应变的改变所引起。于是，可由下面式子求得修正的微量

$$\delta\{\sigma\} = -[D]\delta\{\epsilon\}^p\quad,\quad \delta\{\epsilon\}^p = d\lambda\{\partial f/\partial\sigma\}\quad,\quad \delta\{\alpha\} = C(1-M)\delta\{\epsilon\}^p$$

$$\delta\bar{H} = MH'\delta\bar{\epsilon}^p = MH'd\lambda[(2/3)\{\partial f/\partial\sigma\}]^{1/2} \tag{23}$$

将上述微量迭加到对应的量上，即可求得修正后的应力等值。

3. $\Delta\alpha_z$ 及 $\Delta\epsilon_z$ 的处理 $\Delta\alpha_z \neq 0$，$\Delta\epsilon_z \neq 0$，需要处理。有别于其它文献，在运算中没有引入假设条件。计算流程为: (1) 按 (6) 式计算 $\Delta\alpha_z = C(1-M)\Delta\epsilon_z^{p(i-1)}$ (2) 令三维本构方程中 $\Delta\sigma_z = 0$，可得

$$\Delta\epsilon_z = (D_{13} - X_1)\Delta\epsilon_x + (D_{23} - X_2)\Delta\epsilon_y - X_3 \cdot \Delta\gamma_{xy}/(D_{33} - X_4) \quad (24)$$

$$D_{13} = D_{23} = E\mu/(1+\mu)(1-2\mu) \quad , \quad D_{33} = E(1-\mu)/(1+\mu)(1-2\mu)$$

$$X_1 = 36GS_x(S_x + S_y)/g \quad , \quad X_2 = 36GS_y(S_x + S_y)/g$$

$$X_3 = 36G(S_x + S_y)S_{xy}/g \quad , \quad X_4 = 36G(S_x + S_y)^2/g$$

(3)

$$\Delta\epsilon_z^{pi} = \Delta\epsilon_z + \mu(\Delta\sigma_x + \Delta\sigma_y)/E \quad (25)$$

(4) 若$|\Delta\epsilon_z^{pi} - \Delta\epsilon_z^{p(i-1)}| <$ 允许误差即退出流程，否则返回步骤（1）。

流程开始设 $\Delta\alpha_z = 0$，由（24）、（25）式求得 $\Delta\epsilon^{pi}$ 作为下一流程的 $\Delta\epsilon_z^{p(i-1)}$，重复步骤（1）～（4）到允许误差为止。

五、算例、模拟试验件数值分析

本程序曾对弹性—蠕变、弹塑性—蠕变，变温变载下弹塑性等问题进行考核。

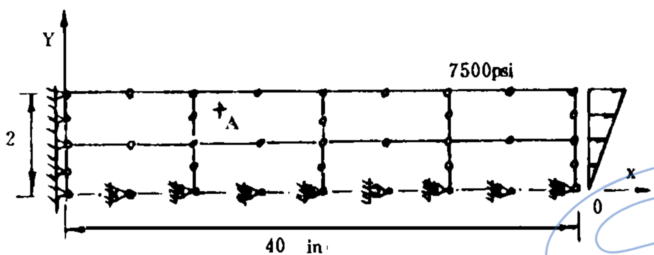

图 2 网格划分

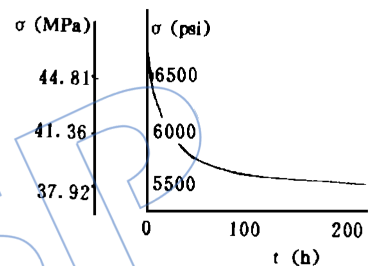

图 3 梁上积分点 A 的应力—时间曲线

例一、一悬臂梁作用弯矩 M，其载荷与材料数据及几何尺寸见文献 [3]，分析蠕变过程应力变化规律。有限元网格划分如图 2，计算的梁上 A 点（30.77，4.54cm）的应力随时间变化曲线如图 3。约 400 小时到达稳态，计算值 39.057MPa，理论值 39.31MPa。

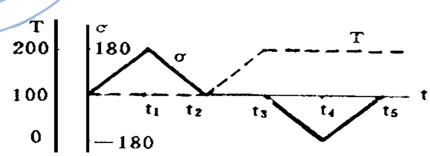

图 4 弹塑性杆的加载条件

例二、一变温变载下的弹塑性杆，材料性质及加载情况如表 1 及图 4 所示。分析不同强化模型的计算结果。所得计算值如表 2 所示，可见计算结果与理论值吻合。

表 1 杆的材料性质

温度	E（MPa）	σ_s（MPa）	H′（MPa）	α（℃）$^{-1}$	μ	M
100℃	120000	120	40000	$.9\times10^{-5}$	.499	.6
200℃	87500	70	20000	$.1\times10^{-4}$	.499	.5

表 2 $\epsilon\times10^2$ 的理论值与计算值

时间	等向强化		随动强化		混合强化	
	理论值	计算值	理论值	计算值	理论值	计算值
t_3	.245	.245005	.245	.245003	.245	.245004
t_4	－.36	－.360696	－.81	－.810427	－.556	－.555598
t_5	－.154	－.154982	－.404	－.404728	－.35	－.349883

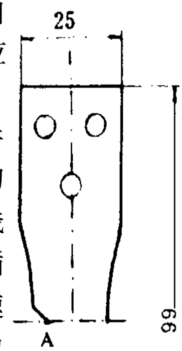

模拟试验件的数值分析模拟试件材料为GH169，采取单边缺口形式，如图 5 所示。在 650℃环境下进行疲劳试验，载荷峰值 19.62KN，已知循环应力应变曲线及蠕变规律，现分析试件危险点 A 的应力应变回线。

计算方案是，按多级疲劳试验的稳态回线得到循环应力应变确定 M，并用稳态蠕变规律求解。按三种波形（$R=-1$ 情况）计算：(1) 无保持时间的三角波。(2) 拉保持时间 1 分钟。(3) 拉保持 3 分钟。点 A 的应力应变回线特点是，对方案 (1) 循环三周后回线稳定，对于方案 (2) 与 (3) 则随着循环次数的增多，得到向右移动的回线如图 6 所示。保持时间长则回线移动速度快，应变幅值大，但随着循环次数的增加移动速度降低、应变幅值与应力幅值均有所减小，并且回线形状逐渐趋向稳定。

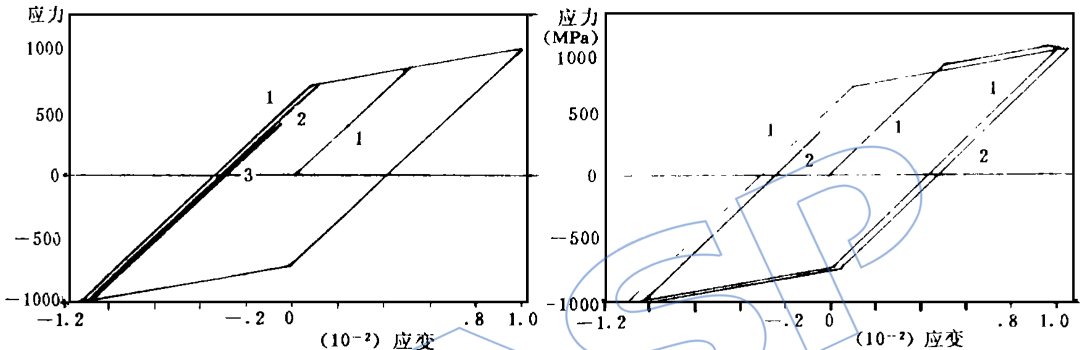

图 6　A 点应力应变曲线（a. 保持 1 分钟；b. 保持 3 分钟）

六、结　　论

1. 程序经考核，计算值与理论值能很好吻合，说明程序可靠、精度高。

2. 程序能对循环加载构件进行应力应变分析，并且计算结果能区分非弹性应变增量各分量，便于考虑蠕变疲劳交互作用的寿命预测使用。

3. 本构关系采用 Prager 线性假设 $d\alpha_{ij}=cd\varepsilon_{ij}^{p}$，一般对 Massing 材料是可行的，对非 Massing 材料，以采用非线性关系为宜，函数的形式需进一步研究。

4. 强化参数 M，一般情况不仅与温度有关还和 ε_p 有关，若根据多级疲劳试验的稳态回线及构件的应力水平范围选取适当的 M 值，能较好地反映实际情况。

参　考　文　献

[1] Mu Xiaying & Zhao Shexu, "A Research on Costitutive Equations of Anisotropic Hardening Material in the Transient Temperature Field", ICCLEM, 1989.

[2] Mu Xiaying & Hu Hurang, "A Finite Element Elastic-Plastic-Creep Analysis of Materials with Temperature Dependent Properties", Computers & Structures, Vol30, No.4, 1988.

[3] Marais N. J. & Martin J. B., "A Solution Algorithm for the Finite Element Analysis of Creep Problem", Eng. Comput, Vol.4, 1987.

a standard deviation of negative three times (-3σ) with the confidence level of 95% and survivability of 99.87%.

3. Finite element methods, especially 3D nonlinear FEM and dynamical FEM for structure analysis have been developed substantially and extensively, and testified experimentally. All of these methods open up broad prospects for FEM application.

4. Besides LCF prediction, a progress has been made in life prediction under the fretting-creep, and creep-fatigue interactions.

5. Achievements in measuring and testing techniques have been also gained so that the effective means and conditions have been provided for experimental research projects.

The AESIRP is still going on. Its further achievements will been compiled in another special issue.

AESIRP SPECIAL ISSUE

MEASUREMENT OF ELASTOPLASTIC STRESSES OF ROTATING DISK IN HOT STATE

Liu Xiangsheng

(***Shengyang Aeroengine Research Institute***)

ABSTRACT The philosophy、the measurement scheme、the essential technological data treatment and the error analysis in the measurement of elastoplastic strains and stresses at median and high temperatures are considered in this paper. The method for identification of plastic state of the disk, as well as the approach to obtaining the secant module and transverse deformation coefficient are presented. The accuracy of the measurements is quite sufficient. The useful measuring and testing technique as well as reference data are provided for the engineering utilization and theoretical analysis.

ANALYSIS OF THERMOELASTOPLASTIC CREEP FINITE ELEMENT UNDER CYCLIC LOADING

Mu Xiaying and Hu Zhiqiang

(***Xian Jiaotong University***)

ABSTRACT The incremental constitutive equations of thermoelastoplastic creep analysis has been derived under the conditions of variable temperatures and loadings. The finite element basic formulation of the plane stress state has been deduced and the program MTEPCA of its thermoelastoplastic creep analysis under cyclic loading has been worked out. Two sophisticated problems in the programming have been tackled. One is how to improve computational accuracy under the influence of various thermoelastoplastic creep factors. For this purpose the subincremental method and the Newton iteration are applied to calculation of the stress and the elastoplastic weight coefficient respectively, besides a high-accurate

method is proposed for yield surface correction. The other is how to deal with $\Delta\alpha_z$ and $\Delta\epsilon_z$ of plane stress problem becauase they are not equal to zero. The solution of this problem is also provided in the program. Several numerical examples are given to check the reliability of the MTEPCA program. The stress-strain hysteresis loops of the point A (danger point) on the analogue sample under cyclic loading are analysed for the structural integrity research.

VARIABLE AMPLITUDE LCF LIFE PREDICTION METHODS

Wang Lüsheng, Ru Meixiu, Cao Fenglan, Gong Mengxian

(***Gas Turbine Establishment***)

ABSTRACT This paper describes our variable amplitude LCF life prediction system based on the strain fatigue theory. The local stress-strain method modified by us is more accurate than the conventional local stress-strain method, This method is provided for disk life design. The presented system is also capable of accurate prediction of the variable amplitude LCF life according to the statistic data of smooth round bar specimen LCF lives to failure, so it is quite a convenient and simple experimental estimation method. Finally, the new method used in the presented system for detemining the reliability life of rotating disks is better than the method in EGD-3 stress standard.

STRESS INTENSITY FACTORS AND THE PROPAGATION OF SURFACE CRACK IN TURBINE DISK

Zheng Guanghua and Xia Deyi

(***Beijing University of Aeronautics and Astronautics***)

ABSTRACT A displacement method is provided to determine the stress intensity factors of nodes on crack surface in cracked body. The K_I at the points along crack front of surface crack are obtained from the curve of K_I versus r by the extrapolation. The K_I of semi-circular and semi-elliptical surface crack in the finite-thickness plates subjected to tensile load are calculated by the three-dimensional finite-element method. The photoelastic experiments with stress frozen method are made to examine the accuracy of the calculated results by the present method. Based on the expression proposed by Elber and Newman for the crack growth rate, the crack growth pattern and the life prediction of semi-elliptical crack in a turbine disk of a jet engine are investigated. It is shown that the method presented in this paper is simple and convenient to analyse surface crack problems of engineering components.

A LARGE ANALYTICAL DEFORMATION METHOD FOR PREDICTION OF DISK BURST SPEED

Hong Qilin and Wang Ping

(***Beijing University of Aeronautics and Astronautics***)

ABSTRACT A new method has been elaborated to predict the burst speed of aeroengine disks. The disks should overspeed or even break due to malfunction of control system, shaft decoupling or afterburning failure. In order to avoid catastrophic failure of an engine, it is required to allow a margin of the disk burst speed. When the maximum rotor speed approaches to the disk burst speed, the plastic strain attains to large value in strain-